Preparation and characterization of magnesium/carbonate co-substituted hydroxyapatites

I. R.GIBSON†, W.BONFIELD*
IRC in Biomedical Materials, Queen Mary, University of London, Mile End Road, London E1 4NS, UK

A new synthesis/processing method has been devised to produce magnesium/carbonate co-substituted hydroxyapatite ceramics that do not decompose to tricalcium phosphate (TCP) on sintering. Using this method, a series of magnesium/carbonate co-substituted hydroxyapatite (Mg/CO_3–HA) compositions, containing between 0 and 0.35 wt % Mg and approximately 0.9 wt % CO_3 were prepared. Sintering the Mg/CO_3–HA compositions in a CO_2/H_2O atmosphere yields a single crystalline phase that appears to be identical to stoichiometric HA. In contrast, when the compositions were prepared in the absence of carbonate and were sintered in air, the phase composition was a biphasic mixture of HA and TCP e.g. for 0.25 wt % Mg substitution the phase composition was approximately 60%HA/40% TCP. Clearly, both the synthesis route and the processing (i.e. sintering) route are of importance in the production of a single-phase Mg/CO_3–HA ceramic. Fourier transform infrared (FTIR) spectroscopy has indicated that the Mg/CO_3–HA ceramics still contained carbonate groups after sintering at 1200 °C. Chemical analysis by X-ray fluorescence spectroscopy (XRF) and C–H–N analysis has shown that the cation/anion molar ratio (i.e. [Ca + Mg]/[P + C/2]) of the different compositions were 1.68(± 0.01), which is equivalent to the Ca/P molar ratio of stoichiometric HA. Although the magnesium/carbonate co-substitution had a positive effect in preventing phase decomposition during sintering, it appeared to have a negative effect on the densification of the Mg/CO_3–HA ceramics, compared to stoichiometric HA.

Introduction

Synthetic hydroxyapatite (HA), $Ca_{10}(PO_4)_6(OH)_2$, is increasingly being used as a bone graft material [1, 2] as an alternative to autograft and allograft bone replacements. HA is osseoconductive *in vivo* [3], which is due largely to the chemical similarity of HA and bone mineral. The rate of remodeling of HA *in vivo* is, however, very slow [4] and consideration of the complex chemistry of bone mineral, compared to synthetic HA, may explain this. Although bone mineral is essentially a calcium phosphate apatite phase, it also contains significant concentrations of other ions [5, 6]. Excluding carbonate ions, the major ''secondary'' ions in bone mineral are sodium and magnesium, with contents typically quoted as being between 0.2 and 1 wt %. These ''secondary'' ions play an important role in the biological/chemical behavior of bone mineral. This has been illustrated by Kakei *et al*. [7], who found that Mg ions were present in a high concentration (approx. 1 wt %) in the bone mineral of new-born rats and that this level decreased with time to a level of 0.5 wt % after 1 year. The chemistry of the bone mineral was clearly related to the formation and growth stages of new bone. In contrast, the authors observed that the carbonate level of the bone mineral was very low at birth, but increased three-fold after only one week. It may be hypothesized that if a hydroxyapatite material was produced that contained comparable levels of these ions, then the behavior of this synthetic material *in vivo* may be more similar to bone mineral, compared to stoichiometric HA. Bigi *et al*. [8] also reported that immature calcified tissue was rich in Mg, with increasing calcification corresponding to a decrease in the Mg content.

A number of studies have reported the synthesis of magnesium-containing hydroxyapatite materials, or magnesium-substituted hydroxyapatite [9–15]. Some of these studies involve the characterization of an as-precipitated material and not a material that has been heat-treated [9–11]. It has been shown that non-heat-treated calcium phosphates produced by aqueous precipitation methods can present a diffraction pattern of a poorly crystalline apatite for Ca/P molar ratios of between 1.50 and 1.67 [16, 17]. It is only when these materials are heat-treated to temperatures greater than 750 °C that the true phase composition, as predicted by the chemical composition, is observed. Therefore, to

*Now at the Department of Materials Science and Metallurgy, University of Cambridge, Pembroke Street, Cambridge, CB2 3QZ, UK.
†Now at the Department of Biomedical Sciences, Institute of Medical Sciences, University of Aberdeen, Foresterhill, Aberdeen, AB25 2ZD, UK.

determine if magnesium substitution in to the HA lattice is possible without compromising phase purity, these materials need to be heat-treated prior to characterization. Studies to date on preparing magnesium substituted hydroxyapatite all observed a similar effect, whereby the magnesium substitution favors the phase decomposition of hydroxyapatite on heating producing a bipbasic mixture of hydroxyapatite and tricalcium phosphate (TCP) [12–15]. This phase decomposition can be explained by considering studies on the incorporation of Mg ions in to the β-tricalcium phosphate (TCP) structure, where it stabilizes the structure [18, 19]. Magnesium substitution stabilizes the β-polymorph of TCP, so that the transformation to the higher temperature α-polymorph occurs at higher temperatures with Mg–TCP than pure TCP [20]. Also, naturally occurring TCP, whitlockite, contains Mg ions substituted for Ca ions. It appears that when Mg is substituted into the HA structure, the more stable phase composition after heat-treatment is that which contains Mg–TCP and HA [21].

In order to substitute Mg ions in to the HA structure and to maintain the phase purity on heat treatment, a different approach is required. Considering other reactions to substitute ionic species into the HA structure, it has been well documented that sodium and carbonate ions can be co-substituted into the HA structure [22–25]. Although magnesium ions have the same charge as calcium ions, whereas sodium ions have a lower charge, magnesium ions are much smaller than calcium or sodium ions. In Na/CO_3 co-substituted hydroxyapatite, the lower charge of the sodium ion is compensated by the carbonate ion having a lower charge than the phosphate group, resulting in overall charge balance. It can be assumed that in order to substitute a smaller Mg ion for a larger Ca ion, some additional structural changes may be needed to prevent destabilization of the structure and subsequent phase decomposition. The co-substitution of a second ionic species would be a simple way of achieving this, as demonstrated for Na/CO_3 co-substituted hydroxyapatite. Some studies have co-substituted magnesium and carbonate ions [10, 11] or magnesium and fluoride ions [26], but the phase stability of these materials after heat-treatment was not reported.

In the present study, a series of magnesium/carbonate co-substituted hydroxyapatite (Mg/CO_3–HA) compositions, containing 0.1, 0.25 and 0.35 wt % Mg and approximately 1 wt % CO_3 were prepared by a simple acid-base precipitation reaction. The phase compositions after heat-treatment/sintering of these Mg/CO_3–HA compositions were compared to similar magnesium compositions but without the co-substitution of carbonate ions and to a stoichiometric HA.

Materials and methods

Sample preparation

The precipitation method was based on the mixing of a suspension of $Ca(OH)_2$ and a solution of H_3PO_4, as described by Akao *et al*. [27]. The magnesium ions were introduced by adding the appropriate quantity of magnesium nitrate to the $Ca(OH)_2$ suspension and carbonate ions were introduced to the reaction mixture by bubbling CO_2 gas in to the H_3PO_4 solution [28]. The amount of H_3PO_4 used remained constant at 0.3 mol for all compositions. The (Ca + Mg) content was adjusted to remain at 0.503 mol for all compositions. This meant that the (Ca + Mg)/P ratio would be greater (1.68) than the stoichiometric value for HA of 1.67; this would allow carbonate groups to be incorporated on to the phosphate sites to try to retain stoichiometry. Carbonate substitution was previously demonstrated in apatites with Ca/P molar ratios greater than 1.67, by a similar process [29]. A range of Mg/CO_3–HA compositions were prepared, containing 0.1, 0.25 and 0.35 wt % Mg.

The above process was repeated, but without the addition of CO_2 gas to the H_3PO_4 solution, producing only Mg–HA compositions. Additionally, a stoichiometric HA was prepared as a reference material by precipitating 0.5 mol of $Ca(OH)_2$ and 0.3 mol of H_3PO_4.

All precipitation reactions were carried out at room temperature and the pH was maintained at 10.5 by the addition of ammonium hydroxide solution. After complete mixing of the reactants, the suspension was aged overnight. The resulting precipitate was filtered, dried at 80 °C overnight and then ground, milled and sieved to a fine powder ($< 75\,\mu m$), as described elsewhere [30].

Characterization techniques

Small amounts of the processed powders (1 g) were pressed into powder compacts using a uniaxial press and a steel die, with an applied pressure of 200 MPa. The powder compacts and portions of the powders (1 g) were sintered in a tube furnace (Carbolite, UK) at 1200 °C for 2 h, with a heating rate of 2.5°/min. For the Mg/CO_3–HA compositions, a sintering atmosphere of CO_2, passed through water, was used.

The calcium, phosphorus and magnesium contents of the different as-precipitated compositions were determined by X-ray fluorescence (XRF) spectroscopy using a Philips PW1606 spectrometer (Ceram Research, UK). The results were quoted as weight percent of the oxides. The carbonate contents of the heat-treated powders were measured by C–H–N analysis (Medac Ltd., UK); the lower limit of detection was less than 0.01 wt % carbon. The phase composition of the heat-treated powders and powder compacts were determined using X-ray diffraction (XRD). A Siemens D5000 diffractometer with Cu K_α radiation was used; the X-ray generator operated at 40 kV and 40 mA. A secondary monochromator was used on the diffracted beam side with a scintillation counter detector. Data were collected over the 2θ range 5–110° with a step size of 0.02° and a count time of 12 s. Identification of phases was achieved by comparing the diffraction patterns of HA and Mg/CO_3–HA with ICDD (JCPDS) standards [31].

Determination of the structural parameters of HA and Mg/CO_3–HA was made by Rietveld refinement of the X-ray diffraction data collected for heat-treated powders. The refinement software GSAS [32] was used and the refinements were based on the structural data for HA of Kay *et al*. [33], using the space group $P6_3/m$. The following parameters were refined: background parameters, scale factor, zero point, lattice parameters,

atomic positions, temperature factors and the OH site occupancy.

Fourier transform infrared (FTIR) spectra were obtained using a Nicolet 800 spectrometer in conjunction with a MTech PAS cell. Spectra were obtained between 4000 and 400 cm^{-1} at 2 cm^{-1} resolution averaging 128 scans. The sample chamber of the PAS cell was purged with helium gas and dried by employing magnesium perchlorate as a drying agent.

The effect of magnesium/carbonate substitution on the densification of HA was assessed by sintering powder compacts of stoichiometric HA and Mg/CO_3–HA at temperatures between 900 °C and 1250 °C. Sintered densities were obtained from the measurement of geometric dimensions and sample mass. For each sintering condition three compacts were sintered and the average value of sintered density was determined. All densities were quoted as a percentage of the theoretical density of HA, 3.156 gcm^{-3} [31]. The microstructures of the sintered disks were examined by scanning electron microscopy (SEM) using a JEOL 6300 SEM; specimens were polished to a 10 μm finish and etched with 5% H_3PO_4.

Results

The results of the chemical analysis of the Mg/CO_3–HA and stoichiometric HA compositions are presented in Table I. The (Ca + Mg)/P molar ratios of all the Mg/CO_3–HA compositions are greater than the design composition of 1.68 and are also greater than that of stoichiometric HA. This higher value implied that there was less phosphate incorporated in the final reaction product that the reactant composition suggested. There was good agreement between the expected and the measured level of magnesium for all compositions. The carbonate content of the heat-treated samples (1000 °C), as measured by C–H–N analysis, was relatively constant for the three Mg/CO_3–HA compositions, with a level of 0.9 ± 0.1 wt %. The heat-treated stoichiometric HA contained no carbonate, as did the heat-treated Mg–HA compositions, within the detection limits of the instrument.

The overall [Ca site]/[P site] molar ratio could be calculated by including the carbonate contents of the samples in to the XRF results. Two different models could be presumed, where either all of the carbonate groups were located on the phosphate site [Ca + Mg]/[P + C], or were divided equally between the phosphate site and the hydroxyl site [Ca + Mg]/[P + C/2]. For the former model, a ratio of approximately 1.65 was observed for all Mg/CO_3–HA compositions, whereas the latter model gave a ratio of approximately 1.68, Table I.

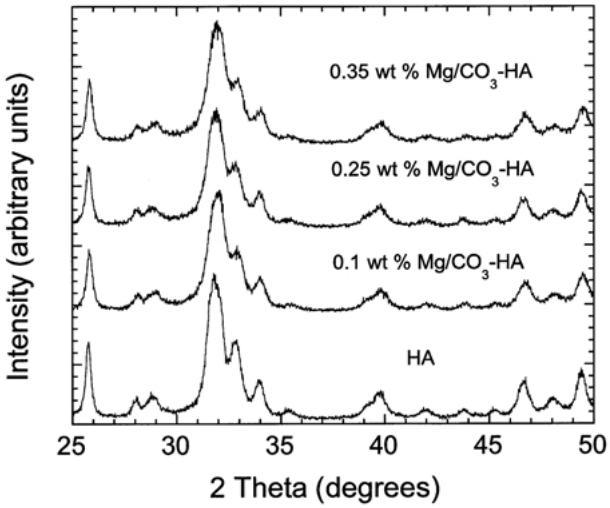

Figure 1 X-ray diffraction (XRD) patterns of as-precipitated magnesium/carbonate co-substituted hydroxyapatite (Mg/CO_3–HA). Increasing the level of substitution results in a small increase in the width of the diffraction peaks, corresponding to a reduction in crystallite size.

X-ray diffraction patterns of the as-precipitated, non-heat-treated HA and Mg/CO_3–HA samples are shown in Fig. 1. Increasing the level of Mg substitution produced broader diffraction peaks, corresponding to a decrease in the crystallite size. No secondary phases were observed in any of the diffraction patterns.

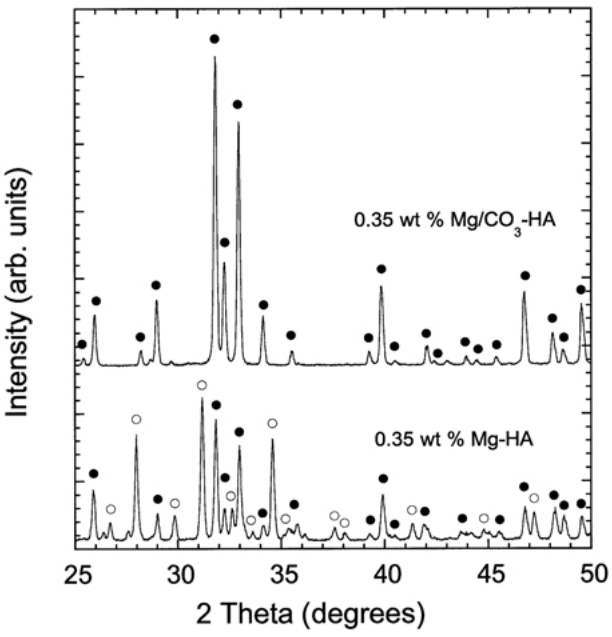

Figure 2 X-ray diffraction (XRD) patterns showing the effect of (a) 0.35 wt % magnesium/carbonate (Mg/CO_3–HA) co-substitution and (b) carbonate-free 0.35 wt % magnesium (Mg-HA) substitution on the phase composition of hydroxyapatite at 1200 °C (CO_2/H_2O atmosphere). • corresponds to HA; ○ corresponds to β-TCP.

TABLE I The results of XRF and CHN analysis of Mg/CO_3–HA and HA samples

Sample ID	[Ca + Mg]/P	wt % Mg (XRF)	wt % CO_3 (1200 °C)	[Ca + Mg]/[P + C]	[Ca + Mg]/[P + C/2]
Stoichiometric HA	1.68	< 0.01	< 0.01	1.68	1.68
0.1 wt % Mg/CO_3–HA	1.70	0.10	0.9	1.65	1.67
0.25 wt % Mg/CO_3–HA	1.70	0.24	1.0	1.65	1.68
0.35 wt % Mg/CO_3–HA	1.70	0.33	0.8	1.66	1.68

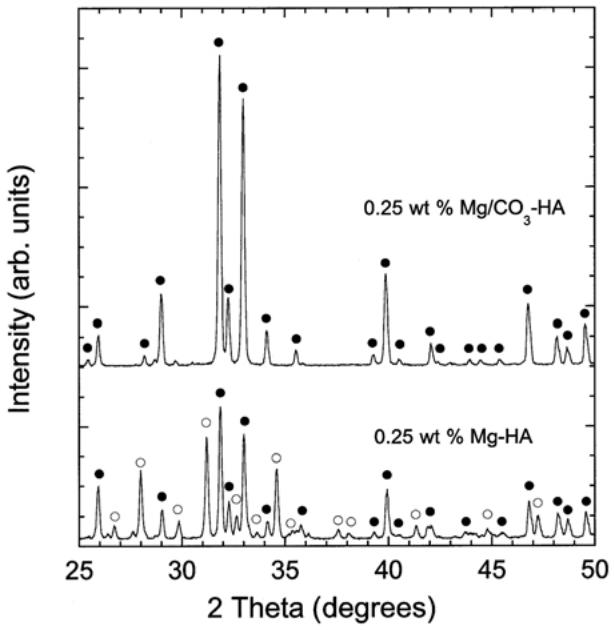

Figure 3 X-ray diffraction (XRD) patterns showing the effect of (a) 0.25 wt % magnesium/carbonate (Mg/CO_3–HA) co-substitution and (b) carbonate-free 0.25 wt % magnesium (Mg-HA) substitution on the phase composition of hydroxyapatite at 1200 °C (CO_2/H_2O atmosphere). • corresponds to HA; ○ corresponds to β-TCP.

The phase compositions of the heat-treated 0.35 wt % Mg/CO_3–HA sample (1200 °C) is presented in Fig. 2 and is compared with a 0.35 wt % Mg–HA sample which does not contain any carbonate groups. The inclusion of carbonate groups helped to retain the phase purity of the Mg/CO_3–HA (i.e. 100% HA-like phase), with only diffraction peaks corresponding to hydroxyapatite present. In contrast, the absence of carbonate in Mg–HA in what is otherwise the same composition results in significant phase decomposition, with a biphasic content of approximately 45% HA-like phase and 55% β-TCP. This effect is observed for all the Mg/CO_3–HA and Mg–HA compositions, with phase pure HA-like compositions obtained for all samples that have carbonate groups included, but phase decomposition to HA + β-TCP mixtures for Mg–HA samples that do not contain carbonate groups. The only difference that is observed is that less β-TCP is obtained for lower Mg contents of Mg–HA compositions, for example, Fig. 3 compares 0.25 wt % Mg/CO_3–HA and Mg–HA compositions, with the latter containing approximately 60% HA-like phase and 40% β-TCP.

The effect of magnesium/carbonate substitution on the unit cell parameters of hydroxyapatite is to cause a significant increase in the *a*-axis and no change in the *c*-axis, when compared to stoichiometric HA, Table II. Although the *a*-axis of the Mg/CO_3–HA samples increased by approximately 0.1% compared to HA, there appeared to be no direct effect of the changing Mg content on the unit cell parameters.

TABLE II The unit cell parameters (± 0.0001) of Mg/CO_3–HA and HA samples sintered at 1200 °C

Sample ID	*a*-axis (nm)	*c*-axis (nm)
Stoichiometric HA	0.9417	0.6878
0.1 wt % Mg/CO_3–HA	0.9429	0.6879
0.25 wt % Mg/CO_3–HA	0.9427	0.6878
0.35 wt % Mg/CO_3–HA	0.9428	0.6878

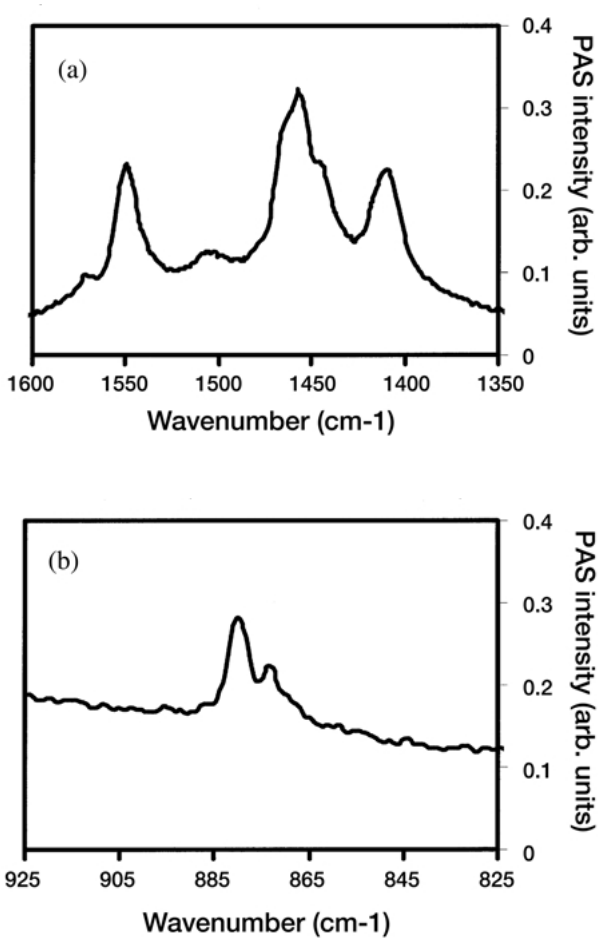

Figure 4 Fourier transform infrared (FTIR) spectra of heat-treated magnesium/carbonate co-substituted hydroxyapatite (0.35 wt % Mg/CO_3–HA) showing the bands corresponding to (a) the ν_3 and (b) the ν_2 modes of the carbonate groups.

FTIR spectra of heat-treated (1200 °C) samples of 0.35 wt % Mg/CO_3–HA showing the bands corresponding to the ν_3 and ν_2 modes are presented in Fig. 4(a) and (b), respectively. The positions of distinct phosphate, carbonate and hydroxide bands of these samples and of 0.25 wt % Mg/CO_3–HA are listed in Table III. The HA sample produces the characteristic phosphate and hydroxyl bands corresponding to synthetic hydroxyapatite [34], and no bands corresponding to carbonate groups were present. In addition to these phosphate and hydroxyl bands, the Mg/CO_3–HA samples also produced bands at approximately 1571, 1550, 1505, 1457, 1446 and 1409 cm^{-1} for the ν_3 mode and at 880 and 873 cm^{-1} for the ν_2 mode. The ratio of the intensities of the two ν_2 bands at 880 and 873 cm^{-1}, which relates the amount of A-type to B-type carbonate substitution, was 2.146. The relative intensity of the hydroxyl stretching band of 0.35 wt % Mg/CO_3–HA at 3571 cm^{-1} was less than that of the hydroxyl band of stoichiometric HA.

The densities of HA and Mg/CO_3–HA ceramics sintered at temperatures between 900 and 1250 °C are presented in Fig. 5. For low sintering temperatures, 900–950 °C, the densities of HA and 0.25 and 0.35 wt % Mg/CO_3–HA samples were comparable. As the sintering

TABLE III Results of FTIR analysis of heat-treated (1200 °C) Mg/CO_3–HA and HA samples; all values correspond to the wavenumbers (cm^{-1}) of the different hydroxyl, carbonate and phosphate bands

	OH	CO_3 ν_3	PO_4	PO_4	CO_3 ν_2	OH	PO_4	PO_4 ν_2
HA	3571	—	1086, 1065 1023	962	—	632	600, 570	473
0.25 wt % Mg/CO_3–HA	3571	1571, 1550 1505, 1457 1446, 1409	1081 1051 1022	962	880 873	631	599, 567	474
0.35 wt % Mg/CO_3–HA	3570	1570, 1550 1505, 1457 1446, 1409	1086 1050 1039	962	880, 873	635	600, 571	473

temperature was increased above 950 °C the densification of HA appeared to be affected by magnesium/carbonate substitution, with lower densities being obtained for the Mg/CO_3 samples for any given sintering temperature. This was most noticeable at approximately 1050 °C where the difference in density of HA and 0.35 wt % Mg/CO_3–HA approached 10% of the theoretical density. As the sintering temperature approached 1250 °C the densities approached similar values, with only 1–2% differences between the HA and Mg/CO_3–HA samples.

The microstructures of the HA and 0.25 wt % Mg/CO_3–HA sample sintered at 1000 and 1200 °C are shown in Figs 6(a), (b) and 7(a), (b), respectively. At 1000 °C, the Mg/CO_3–HA sample exhibited an early stage of sintering, with only small regions of densification of particles. The HA sample showed a greater degree of sintering of particles, with a number of dense regions being visible; the HA particles also appeared to be larger than the Mg/CO_3–HA particles. Sintering at 1200 °C produced a bimodal distribution of grains for both samples, although the Mg/CO_3–HA sample produced an overall smaller grain size than the HA sample. There appeared to be more porosity present in the Mg/CO_3–HA sample, which correlates with the sintered densities displayed in Fig. 5.

Discussion

The synthesis route used was successful in retaining the desired amount of magnesium in the final product (Table I). The method of introducing carbonate into the reaction mixture ensured that there was an excess of these groups available for substitution. XRF analysis of the final products showed that there was less phosphate groups present, as indicated by the higher than expected

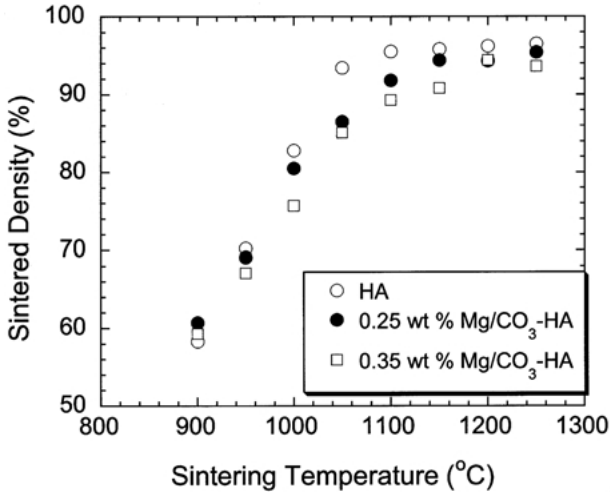

Figure 5 Change in the sintered densities (expressed as a percentage of the theoretical density of HA) of Mg/CO_3–HA and HA for sintering temperatures between 900 and 1250 °C.

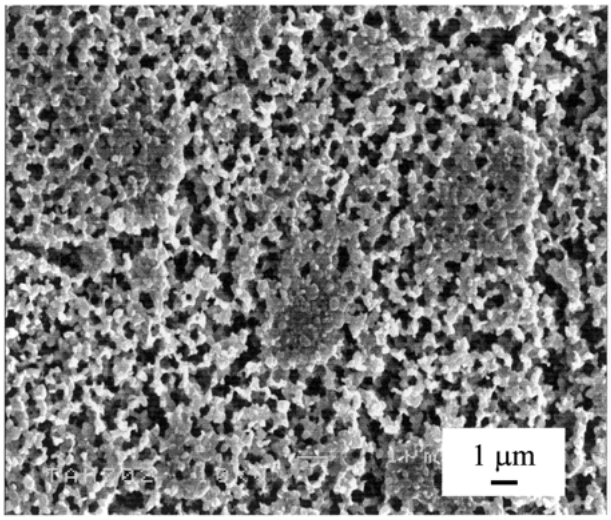

(a)

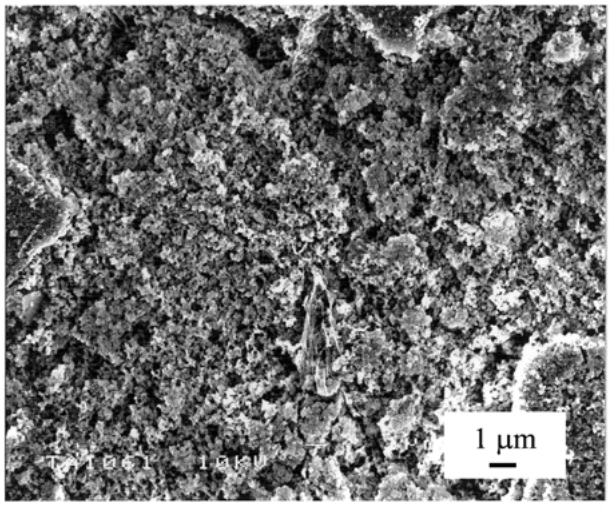

(b)

Figure 6 Scanning electron microscopy images of (a) HA and (b) 0.25 wt % Mg/CO_3–HA sintered at 1000 °C, respectively.

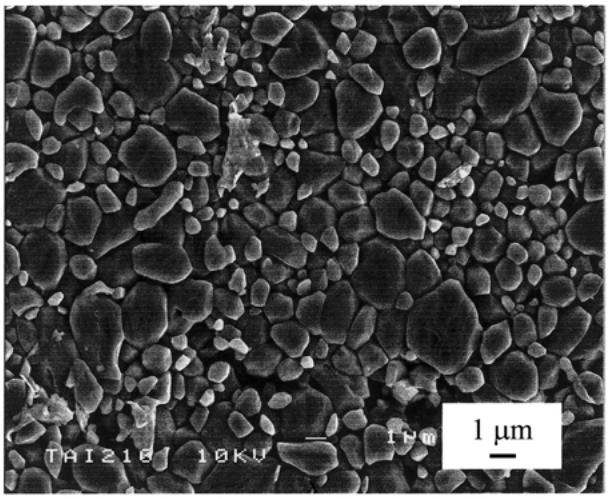

(a)

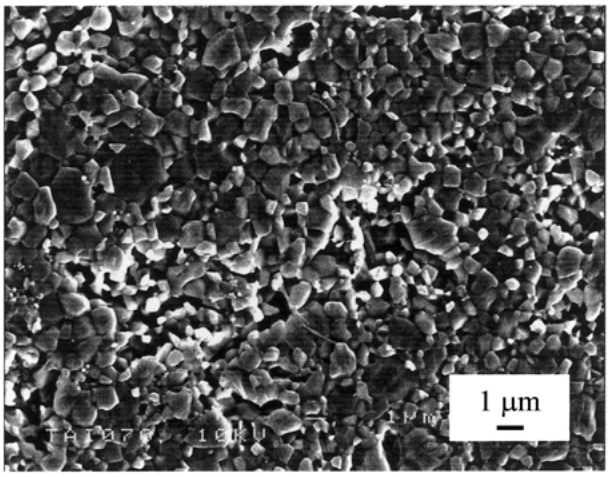

(b)

Figure 7 Scanning electron microscopy images of (a) HA and (b) 0.25 wt % Mg/CO_3–HA sintered at 1200 °C, respectively.

[Ca + Mg]/P ratio, than the initial reactant composition would have suggested. This implied that during synthesis, carbonate groups were incorporated into the phosphate site of the forming apatite composition. On sintering, all Mg/CO_3–HA compositions contained approximately 0.9 ± 0.1 wt % CO_3 which affected the overall molar ratio of (Ca position)/(P position), and this ratio depended on the relative distribution of the carbonate groups over the phosphate (B-type substitution) and hydroxyl (A-type substitution) groups. The relative distribution will depend on the substitution mechanism that allows the co-substitution of Mg and CO_3 ions. The co-substitution of Na and CO_3 ions can be considered as a more straightforward mechanism, as the addition of equal amounts of the two groups ensures that charge balance in the final product is maintained [22, 25]. Magnesium ions, however, have the same charge as calcium ions, so the role of the co-substitution of CO_3 ions is not preserving charge balance. For this reason, the carbonate (CO_3^{2-}) groups that are incorporated in the Mg/CO_3–HA compositions can not be situated exclusively on the phosphate (PO_4^{3-}) positions, as this would result in incomplete balance of charge. Considering the chemical analysis results alone, Table I, also suggested that substitution of carbonate exclusively on the phosphate position was not feasible as this resulted in a [Ca + Mg]/[P + C] molar ratio of approximately 1.65 for all Mg/CO_3–HA compositions, which is lower than the stoichiometric HA. This low (cation)/(anion) molar ratio would result in phase decomposition to HA + TCP during heat-treatment, as would be observed for a Ca-deficient apatite with a Ca/P molar ratio of 1.65; this was not observed by XRD (Figs. 2 and 3). Recalculating the molar ratio by assuming that the carbonate groups are distributed equally over the phosphate and hydroxyl positions produces a [Ca + Mg]/[P + C/2] ratio of approximately 1.68 for all three Mg/CO_3–HA compositions, which is equivalent to the value obtained for the phase-pure stoichiometric HA produced in this study as a reference (Table I). Splitting the carbonate group over two sites (mixed AB-type) also allows charge balance to be maintained, as shown in mechanism (1).

$$[Ca_{10-y}Mg_y][(PO_4)_{6-x}(CO_3)_x][(OH)_{2-x}(CO_3)_x] \quad (1)$$

There does not initially appear to be a direct relationship between the amount of magnesium (y) and the amount of carbonate (x) that is incorporated, but as the two are not mutually required to maintain charge balance, the amount of carbonate incorporated is associated to the [Ca + Mg]/P molar ratio of the initial reaction mixture. For all three Mg/CO_3–HA compositions, this value was designed to be maintained at a constant value of approximately 1.68, and XRF analysis showed that the actual value remained constant at 1.70, and this may explain why a relatively constant value of carbonate ions was incorporated in all three compositions. As the ratio [Ca + Mg]/P was determined to be 1.70, the value of x in mechanism (1) can be determined, and $x = 0.118$. This corresponds to a value of approximately 1.4 wt % carbonate, which is of a comparable order to the measured values in Table I. Chemical analysis of Mg-substituted apatites produced by other methods showed the values of [Ca + Mg]/P molar ratio were less than the stoichiometric value of 1.67 for HA [11, 13, 15], e.g. Yasukawa reported values ranging from 1.25–1.62 [13].

It should be noted that substitution of the carbonate groups exclusively on the hydroxyl position would, as for exclusive substitution on the phosphate group, result in charge imbalance and also would produce a very high molar ratio of approximately 1.70 (Table I).

Analysis of the as-precipitated, non-heat treated Mg/CO_3–HA compositions by X-ray diffraction revealed that Mg substitution had a small effect on the crystallinity of the HA. This was also observed by numerous other studies on non-heat treated Mg-substituted hydroxyapatite/apatite [9–15], although the effects were greater in these studies due to the much higher levels of Mg substitution investigated. It has been established that Mg ions can inhibit the crystallization and growth of hydroxyapatite [15, 35]. The X-ray diffraction analysis of the Mg/CO_3–HA compositions in the present study suggested that the Mg substitution affected the growth of the HA crystals, which was observed as broader diffraction peaks.

The most interesting result obtained in this study was the difference in the phase compositions of the

Mg/CO_3–HA materials compared to Mg–HA materials, which were prepared without carbonate ions being added during synthesis and were sintered in air. The only difference in the two materials was the incorporation of carbonate groups in to the structure of the former material. This actually resulted in the Mg–HA materials having a higher [Ca position]/[P position] molar ratio than the Mg/CO_3–HA materials, but the carbonate-free materials decomposed during sintering. The level of phase decomposition was, however, much greater than would be expected, with a biphasic mixture of approximately 50% HA/50% β-TCP, Figs. 2 and 3; for a non-substituted calcium phosphate material, this phase composition would correspond to a Ca/P molar ratio of approximately 1.58 [36]. The Mg/CO_3–HA compositions, however, produced diffraction peaks corresponding only to the ICDD (JCPDS) standard for HA [31]. The incorporation of carbonate ions in to the HA structure are obviously essential to retain the phase purity of HA when Mg ions are substituted for Ca ions. Bigi *et al*. [15] showed that Mg substitution resulted in phase decomposition of HA when heated to 500 °C or greater, resulting in a biphasic mixture of HA and magnesium stabilized β-tricalcium phosphate. Similar phase decomposition was observed for Mg/CO_3-substituted HA by LeGeros *et al*. [9] heated at 800 °C and by Mayer *et al*. [14] heated above 700 °C, and for a Mg-substituted HA by Yasukawa *et al*. [13] heated above 800 °C. All of these reported thermal treatments were, however, carried out in an air atmosphere, whereas the Mg/CO_3–HA compositions in the present study were heat-treated/sintered in a CO_2 atmosphere.

Measurement of the lattice parameters of heat-treated samples in the present study showed that magnesium and carbonate co-substitution resulted in a uniform increase in the *a*-axis (from 0.9417 nm for HA to 0.9427–0.9429 nm for Mg/CO_3–HA) but no change in the *c*-axis (0.6787 nm), compared to stoichiometric HA. The fact that the unit cell parameters did not change for the different levels of magnesium substitution suggested that the incorporation of the Mg ions did not control the change. This implies that the change was due to carbonate substitution, especially as the same increase in the *a*-axis was observed for all Mg/CO_3–HA compositions. Some studies have reported the unit cell parameters of Mg-substituted HA, although these were determined on materials that had not been heat-treated [11, 13–15]. Mayer *et al*. [14] calculated unit cell parameters for as-prepared Mg-substituted apatite and Mg/CO_3-substituted apatites. For the Mg-only substituted HA samples, they observed a small decrease in both *a* and *c* parameters as the level of Mg substitution was increased. A similar decrease in both *a* and *c* parameters was observed for the Mg/CO_3-substituted apatites, with the changes appearing to be caused by the increasing Mg content and not the presence of CO_3. Bigi *et al*. [15] showed that the *a*-axis did not change significantly but the *c*-axis showed a large decrease with increasing Mg substitution. Yasukawa *et al*. [13] observed a linear decrease in both *a*- and *c*-axis of as-prepared Mg-substituted apatite with increasing Mg substitution. It is difficult to compare the results obtained from heat-treated samples in the present study with these literature values for non-heat-treated samples. Another significant difference between literature values and those obtained here are the levels of magnesium substitution used. In the present study, the maximum Mg substitution is 0.35 wt %, which corresponds to a molar ratio of Mg/(Mg + Ca) of 0.015, whereas studies such as Yasukawa *et al*. [13] prepared compositions that had Mg/(Mg + Ca) ratios of up to 0.55. These results show clearly that high levels of Mg substitution/incorporation are only possible in as-precipitated, non-heat-treated materials and that when these materials are heat-treated they exhibit extensive phase decomposition. To maintain phase stability of Mg-substituted HA on heating, the levels of Mg substitution must be low, carbonate ions need to be co-substituted in the HA structure, and they need to be sintered in a CO_2 environment.

Studies on the co-substitution of sodium and carbonate ions have shown that the unit cell parameters of as-precipitated carbonate substituted HA changes as the level of carbonate substitution changes; LeGeros [37] and Barralet [38] have shown that the *a*-axes decreases and the *c*-axis increases with increasing carbonate substitution on the phosphate site. Studies have also shown that the reverse occurs when carbonate is substituted for hydroxyl groups (A-type), with an increase in a-axes and a decrease in *c*-axis.

Fourier transform infrared (FTIR) spectroscopy is a useful method to investigate the presence and position of carbonate groups in hydroxyapatite [39]. The Mg/CO_3 co-substitution did not appear to affect significantly the positions of the phosphate and hydroxyl bands in the FTIR spectra of HA, Table III. For the Mg/CO_3–HA compositions, carbonate bands were observed for ν_3 mode at approximately 1571, 1550, 1505, 1457, 1446 and 1409 cm^{-1} and for the ν_3 mode at 880 and 873 cm^{-1}. There are contradicting reports in the literature relating the positions of these carbonate bands and the position of the carbonate group in the HA structure, i.e. A-type or B-type [24, 34, 38, 39]. This can lead to difficulties in quantifying the carbonate substitution, but some agreement can be made with the results obtained by LeGeros [39] for A- and B-type carbonate substituted hydroxyapatites. This study showed that A-type substitution produced bands at 1550, 1525, 1460 and 877 cm^{-1} whereas B-type substitution produced bands at 1540, 1450, 1410 and 870 cm^{-1}. There appears to be some correlation between the results obtained for the Mg/CO_3–HA compositions in the present study and the results of LeGeros for both A- and B-type substitution, which would support the proposed mechanism described earlier. Comparing the ν_3 bands of 0.35 wt % Mg/CO_3–HA with those of an AB-type carbonate substituted HA with approximately equal amounts of A : B type substitution [29] shows a significant increase in the relative intensity of the band at 1550 cm^{-1} and a large decrease in the relative intensity of the band at 1409 cm^{-1} for the Mg/CO_3–HA material. Using the data of LeGeros, this would correspond to a greater proportion of A-type carbonate substitution in the Mg/CO_3–HA. This was also evident by the higher than unity ratio of the intensities of the two bands corresponding to the ν_2 vibration from the carbonate group at 880 and 873 cm^{-1}. Although the

FTIR data presented in Fig. 4 implies that there is a greater relative amount of A-type carbonate substitution than is described earlier in Mechanism (1) and Table I, it should be noted that C–H–N analysis was carried out on samples sintered at 1000 °C, whereas the FTIR data was obtained from samples sintered at 1200 °C. Sintering at a higher temperature in a CO_2 atmosphere will increase the possibility of further substitution of some of the hydroxyl groups for carbonate groups, which in turn would not affect the [Ca site]/[P site] ratio.

Although the FTIR data shows clearly that the Mg/CO_3–HA compositions contain both A- and B-type carbonate substitution, it is surprising that there was no band identified at approximately 755 cm^{-1}, which has been associated with A-type carbonate substitution [40]. A similar decrease in the intensities of the hydroxyl bands at 3572 and 630 cm^{-1} with increasing Mg substitution was observed by Bigi *et al*. [15] and Yasukawa *et al*. [13] for non-heat-treated Mg-substituted apatite. It should be noted that $MgCO_3$, a possible phase impurity in this system, produces two strong bands at 1481 and 1419 cm^{-1}, which were not observed for the materials in this study.

Although magnesium/carbonate co-substitution does not appear to affect the phase composition of heat-treated/sintered hydroxyapatite, there have been clear changes in the chemistry of the material as a result of these substitutions. Other ionic substitutions in hydroxyapatite, such as sodium/carbonate [38], ammonium/carbonate [41], silicon [42] and fluoride [43], have all been shown to affect the densification of hydroxyapatite. The results presented in Fig. 5 comparing the densification of the Mg/CO_3–HA compositions with stoichiometric HA showed that the co-substitution had the small negative effect of retarding the densification, relative to HA, at intermediate temperatures (950°–1150 °C). For sintering temperatures higher than 1150 °C the sintered densities became more comparable. This negative effect was slightly surprising considering reported densification data obtained for sodium/carbonate co-substituted HA [38, 41, 44, 45], which showed that the temperature required to achieve near-theoretical densities for these materials was up to 200 °C less than for HA. It should be noted, however, that the sodium and carbonate levels in these materials were much higher than the magnesium and carbonate levels reported here. The low carbonate content, 0.9 wt %, is particularly different, as the sodium/carbonate co-substituted HA materials had typical carbonate contents between 5 and 15 wt %.

The differences in densification behavior observed for HA and Mg/CO_3–HA samples was also reflected in the microstructures of sintered specimens. Although sintered specimens of Mg/CO_3–HA produced higher levels of porosity than stoichiometric HA, a smaller grain size was obtained for Mg/CO_3–HA than for HA for any given sintering temperature. Correia *et al*. [11] studied the effect of two different levels of magnesium substitution on the densification of HA. Although they also observed that Mg substitution inhibited the densification compared to stoichiometric HA, their materials decomposed extensively to β-TCP/HA on sintering. The authors attributed this difference in densification to the formation of the secondary phase during sintering. The same explanation can not be used to describe the results observed in the present study, as no phase decomposition was observed on sintering.

Conclusions

Using an alternative reaction route, a magnesium-containing hydroxyapatite has been prepared that retains phase purity during heat treatment up to 1250 °C. It has been demonstrated that this has been possible by the co-substitution of magnesium (up to 0.35 wt %) and carbonate ions (0.9 wt %) in to the hydroxyapatite lattice. Materials that were prepared with exactly the same (Ca + Mg)/P ratios, but in the absence of carbonate ions, decomposed extensively on heating to produce biphasic mixtures of approximately equal amounts of β-TCP and HA. For the co-substituted Mg/CO_3–HA compositions, results of chemical analysis favored the carbonate ions being located on both the phosphate and the hydroxyl groups. In contrast to hydroxyapatites that have been co-substituted with sodium and carbonate, there was no beneficial effect of Mg/CO_3 co-substitution on the densification of HA. As a result of being able to produce Mg/CO_3–HA ceramics that do not decompose on heating, it will now be possible to study how these biologically relevant ions affect the biological response of hydroxyapatite, without additional complicating factors such as the presence of large amounts of secondary calcium phosphate phases.

Acknowledgments

The support of the Engineering and Physical Sciences Research Council for funding of the IRC in Biomedical Materials is gratefully acknowledged. The authors would also like to thank Mr Bob Whitenstall for assistance with the SEM analysis.

References

1. Y. L. LIU, J. SCHOENAERS, K. DE GROOT, J. R. DE WIJN and E. SCHEPERS, *J. Mater. Sci. Mater. in Med.* **11** (2000) 711.
2. T. KOBAYASHI, S. SHINGAKI, T. NAKAJIMA and K. HANADA, *J. Long-Term Effects of Med. Impl.* **3** (1993) 283.
3. A. MORONI, V. L. CAJA, E. L. EGGER, L. TRINCHESE and E. Y. S. CHAO, *Biomaterials* **15** (1994) 926.
4. C. P. A. T. KLEIN, A. A. DRIESSEN, K. DE GROOT and A. VAN DEN HOOFF, *J. Biomed. Mater. Res.* **17** (1983) 769.
5. A. BIGI, G. COJAZZI, S. PANZAVOLTA, A. RIPAMONTI, N. ROVERI, M. ROMANELLO, K. NORIS SUAREZ and L. MORO, *J. Inorg. Biochem.* **68** (1997) 45–51.
6. F. C. M. DRIESSENS, *Bull Soc. Chem. Belg.* **89** (1980) 663.
7. M. KAKEI, H. NAKAHARA, N. TAMURA, H. ITOH and M. KUMEGAWA, *Ann. Anat.* **179** (1997) 311.
8. A. BIGI, E. FORESTI, R. GREGORININ, A. RIPAMONTI, N. ROVERI and J. S. SHAH, *Calcif. Tissue Int.* **50** (1992) 439.
9. R. Z. LEGEROS, R. KIJKOWSKA, C. BAUTISTA and J. P. LEGEROS, *Conn. Tissue. Res.* **33** (1995) 203.
10. J. D. B. FEATHERSTONE, I. MAYER, F. C. M. DRIESSENS, R. M. H. VERBEECK and H. J. M. HEIJLIGERS, *Calcif. Tissue Int.* **35** (1983) 169.
11. R. N. CORREIA, M. C. F. MAGALHÃES, P. A. A. P. MARQUES and A. M. R. SENOS, *J. Mat. Sci. Mater. in Med.* **7** (1996) 501.

12. K. TÔNSUAADU, M. PELD, T. LESKELÄ, R. MANNONEN, L. NIINISTÖ and M. VEIDERMA, *Thermochimica Acta* **256** (1995) 55.
13. A. YASUKAWA, S. OUCHI, K. KANDORI and T. ISHIKAWA, *J. Mater. Chem.* **6** (1996) 1401.
14. I. MAYER, R. SCHLAM and J. D. B. FEATHERSTONE, *J. Inorg. Biochem.* **66** (1997) 1.
15. A. BIGI, G. FALINI, E. FORESTI, M. GAZZANO, A. RIPAMONTI and N. ROVERI, *ibid.* **49** (1993) 69.
16. K. ISHIKAWA, P. DUCHEYNE and S. RADIN, *J. Mater. Sci. Mater. in Med.* **4** (1993) 165.
17. I. R. GIBSON, I. U. REHMAN, S. M. BEST and W. BONFIELD, *ibid.* **11** (2000) 533.
18. B. DICKENS, L. W. SCHROEDER and W. E. BROWN, *J. Solid State Chem.* **10** (1974) 232.
19. D. CLEMENT, J. M. TRISTAN, M. HAMAD, P. ROUX and J. G. HEUGHEBAERT, *ibid.* **78** (1989) 271.
20. J. ANDO, *Bull. Chem. Soc. Japan* **31** (1958) 201.
21. R. Z. LEGEROS, *Prog. Crystal Growth Charact.* **4** (1981) 1.
22. D. G. A. NELSON and J. D. B. FEATHERSTONE, *Calc. Tiss. Int.* **34** (1982) S69.
23. R. Z. LEGEROS, O. R. TRAUTZ, J. P. LEGEROS and E. KLEIN, *Bull. Soc. Chim. France* (1968) 1712.
24. M. VIGNOLES, G. BONEL and R. A. YOUNG, *Calcif. Tissue Int.* **40** (1987) 64.
25. M. VIGNOLES, G. BONEL, D. W. HOLCOMB and R. A. YOUNG, *ibid.* **43** (1988) 33.
26. M. OKAZAKI, *Biomaterials* **12** (1991) 831.
27. M. AKAO, H. AOKI and K. KATO, *J. Mat. Sci.* **16** (1981) 809.
28. I. R. GIBSON and W. BONFIELD, ''Process for the Preparation of Magnesium and Carbonate Substituted Hydroxyapatite'', International Patent Application No. PCT/GB98/03817.
29. *Idem., J. Biomed Mater. Res.* **59** (2002) 697.
30. I. R. GIBSON, S. KE, S. M. BEST and W. BONFIELD, *J. Mat. Sci. Mater. In Med.* **12** (2001) 163.
31. PDF Card no. 9-432, ICDD, Newton Square, Pennsylvania, U.S.A.
32. A. C. LARSON, R. B. VON DREELE and M. LUJAN Jr., GSAS – Generalised Crystal Structure Analysis System, Neutron Scattering Centre, Los Alamos National Laboratory, California (1990).
33. I. KAY, R. A. YOUNG and A. S. POSNER, *Nature* **204** (1964) 1050.
34. I. REHMAN and W. BONFIELD, *J. Mat. Sci. Mater. Med.* **8** (1997) 1.
35. A. A. CAMPBELL, M. LOROE and G. H. NANCOLLAS, *Colloids and Surfaces* **54** (1991) 25.
36. A. SLÓSARCZYK, E. STOBIERSKA, Z. PASZKIEWICZ and M. GAWLICKI, *J. Am. Ceram. Soc.* **79** (1996) 2539.
37. R. Z. LEGEROS, *Nature* **205** (1965) 403.
38. J. BARRALET, PhD Thesis, University of London, UK (1995).
39. R. Z. LEGEROS, O. R. TRAUTZ, E. KLEIN and J. P. LEGEROS, *Experimentia* **25** (1969) 5.
40. H. EL FEKI, C. REY and M. VIGNOLES, *Calc. Tiss. Int.* **49** (1991) 269.
41. Y. SUWA, H. BANNO, H. SAITO, Y. DOI, T. KODA, M. ADACHI and Y. MORIWAKI, in ''Bioceramics'', Vol. 6, edited by P. Ducheyne and D. Christiansen (Butterworth-Heinemann Ltd., Oxford, 1993) 381–386.
42. I. R. GIBSON, S. M. BEST and W. BONFIELD (submitted *J. Am. Ceram. Soc.* 2001).
43. N. SENAMAUD, D. BERNACHE-ASSOLLANT, E. CHAMPION, M. HEUGHEBAERT and C. REY, *Solid State Ionics* 101–103 (1997) 1357.
44. Y. DOI, T. KODA, M. ADACHI, N. WAKAMATSU, T. GOTO, H. KAMEMIZU, Y. MORIWAKI and Y. SUWA, *J. Biomed. Mater. Res.* **29** (1995) 1451.
45. J. C. MERRY, I. R. GIBSON, S. M. BEST and W. BONFIELD, *J. Mat. Sci. Mater. Med.* **9** (1998) 779.

Received 14 May
and accepted 23 October 2001